

Base and additive free click chemistry strategy to accomplish the synthesis of amalgamated pyrazolo-triazole heterocyclic scaffolds and their molecular docking study

Ashok Waskle^a, Dharamsingh Waskle^a, Twinkle Solanki^a, Prakash Barfa^a, Pratibha Sharma^a and Ashok Kumar^{a*}

^aSchool of Chemical Sciences, Devi Ahilya Vishwavidyalaya, Indore (M.P.)-452001, India

CHRONICLE

Article history:

Received February 25, 2024

Received in revised form

March 25, 2024

Accepted July 3, 2024

Available online

July 3, 2024

Keywords:

Click Chemistry

Copper Catalyst

1, 2, 3-Triazole linked

Pyrazolone

Molecular Docking

ABSTRACT

The current work involves the synthesis of amalgamated heterocyclic scaffolds embracing pyrazolone and triazole nuclei. The suggested methodology leads to streaming in the targeted synthesis in a multicomponent reaction manner resulting in 91% yield of the structural motifs. This strategy makes use of the click reaction mechanism of copper-catalyzed azide-alkyne (CuAAC) cycloaddition. The structures of all the synthesized compounds were ascertained considering spectro-analytical data from ¹H NMR, ¹³C NMR, and FTIR and Mass studies. Subsequently, molecular docking studies were performed taking into account the *P. gingivalis* as the heme binding targeted protein.

© 2025 by the authors; licensee Growing Science, Canada.

1. Introduction

The triazole scaffold has been noticed as the core integral moiety in the variegated domain of azaheterocycles.^{1, 2} The development of new synthetic protocols enabling rapid and straightforward access to this heterocyclic scaffold is the key focus of current research and development scenario³⁻⁵. In this context, the click chemistry approach has become one of the leading strategies in the current synthetic chemistry domain.⁶⁻⁸ The approach is highly efficient and reliable with a wider scope, high productivity, and operational simplicity under benign conditions with easy product isolation.⁹ Specifically, the copper-catalyzed azide-alkyne cycloaddition (CuAAC) represents an excellent contribution to transition metal catalysis in synthetic organic chemistry.^{10,11} The efforts of Sharpless¹² and Meldal¹³ made copper-catalyzed azide-alkyne cycloaddition (CuAAC) reaction as a prime example of “Click Chemistry” for assembling complex molecules which are widely used in organic chemistry,¹⁴ polymer chemistry, material science,¹⁵ pharmaceutical chemistry and biological conjugation.¹⁶

Furthermore, the Cu-catalysed cycloaddition of alkynes with azide could afford a number of substituted 1, 2, 3-triazoles.^{17, 18} Such substituted triazoles and their derivatives are key components of many skeletal frameworks of biologically active molecules.¹⁹⁻²² Moreover, the synthesis of triazole coupled to other heterocyclic nuclei has attracted greater attention because of the augmented pharmacological profile of the hybrid skeleton.²³ Their derivatives possess a number of vital biological activities. *viz* antibacterial,²⁴ anti-viral, anti-fungal,²⁵ anti-cancer, anti-depressant, anti-inflammatory,²⁶ antipyretic, and anti-convulsant activities.²⁷ Henceforth, considering aforementioned discussion and in continuation of our work in the domain of heterocyclic synthesis,²⁸⁻³⁵ herein we attempted to report the synthesis of a new series of hetero-bicyclic scaffolds involving click reactions between terminal alkynes and azides. Initially, a series of N-

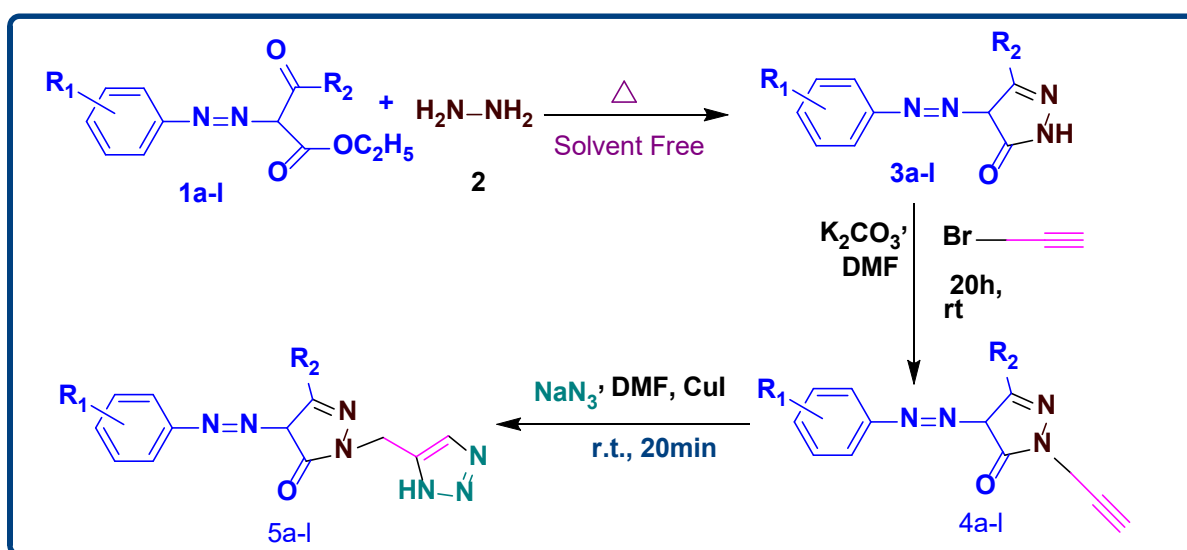
* Corresponding author

E-mail address drashoksharma2001@yahoo.com (A. Kumar)

alkenyl-arylazo pyrazolone was synthesized as one of the synthetic equivalents. Subsequently, azidation of the precursor leads to the generation of substituted triazole derivatives.

The most straightforward method for creating 1, 2, 3-triazoles involves the azide molecular segment participating in non-catalyzed cycloaddition reactions. Recent literature has delved into various aspects of this process, particularly focusing on the questions of region-selectivity, kinetics, and the underlying mechanisms of numerous thermal azide cycloaddition examples. These studies aim to elucidate the factors that influence the selective formation of triazole isomers and the rates at which these reactions proceed. After understanding the mechanistic pathways and kinetic parameters, researchers can better control and optimize the synthesis of 1,2,3-triazoles, which are valuable compounds in pharmaceuticals and materials science.³⁶⁻³⁸

The Cu-catalyzed approach to cycloaddition is particularly effective for reactions involving non-activated 2π -components. This method enhances region-selectivity, which is typically low in non-catalyzed transformations, thereby allowing for more precise and predictable product formation. The catalytic action of copper facilitates the cycloaddition process, leading to higher yields and cleaner reactions compared to thermal methods.³⁹ An overview of a synthetic scheme of triazole-linked pyrazolone is delineated in **scheme 1**.

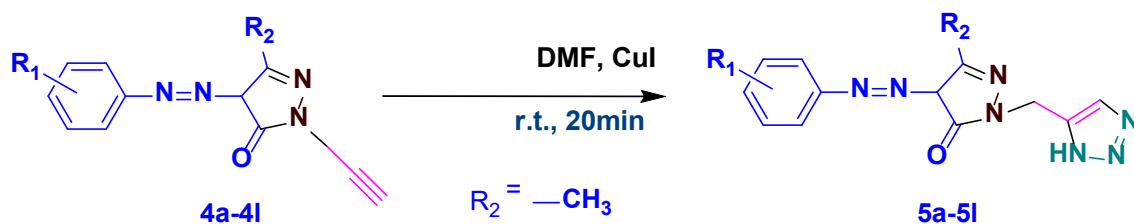


Scheme 1. Synthesis of triazole-linked pyrazolone.

The objective of these studies is to develop an efficient and environmentally friendly comprehensive investigation into a base and additive-free click chemistry strategy for the synthesis of amalgamated pyrazolo-triazole heterocyclic scaffolds. Consequently, we seek to contribute to the advancement of synthetic methodologies and the understanding of molecular interactions with the goal of exploring novel compounds with pharmacological significance.

2. Results and Discussion

A series of substituted 1, 2, 3-triazoles embracing both electron-withdrawing and electron-donating groups was synthesized under optimized reaction conditions. Optimization studies assess the feasibility of a reaction in terms of the role of different solvents, catalysts, reaction time and temperature. To evaluate the role of different solvents, the reaction was performed in various solvents such as dichloromethane, dimethylformamide, dichloroethane, chloroform, methanol and ethanol. These optimizations revealed the use of polar protic solvents such as methanol and ethanol to be unsuitable on account of very low product yields. However, the use of polar-aprotic and non-polar solvents gave appreciable yield of the desired product. It was inferred that among all the solvents used, DMF was found to be the optimal for this reaction to result in maximum yield (**Fig. 1**). Hence, considering this in view, the reaction was performed in dimethylformamide with 5 mol% loading of CuI as the catalyst. Likewise, the optimization study of temperature and time has revealed 20 minutes of reaction time at room temperature as the optimized parameters required to yield the final product. Increase of temperature from 50 to 90 °C resulted in decreased product yield with two-to-three-fold increase in reaction time. These optimizations were carried out by regular monitoring of the reaction through TLC studies. Increase in temperature resulted in diminishing the yield of product for all the compounds optimized. Compounds with *para*-chloro substituent resulted in the decrease in the yield of product from 87% to 65% while the compounds with *para*-methoxy substituent resulted in the decrease from 88% to 62%. However, yield of *para*-nitro substituent resulted in a slight decrease with simultaneous reaction time increase in to twice to that of reaction carried out at room temperature. An overview of optimization studies is given in **Table 1** and **Table 2**.

Table 1. Optimization study of reaction time and temperature examined for different substituents.

| Entry | R ₁ | Product | Time(min) | Temperature | Yield (%) |
|-------|--------------------|---------|-----------|-------------|-----------|
| 1 | 4-NO ₂ | 5a | 20 | rt | 91 |
| 2 | 4-NO ₂ | 5a | 40 | rt | 91 |
| 3 | 4-NO ₂ | 5a | 40 | 50 | 80 |
| 4 | 4-NO ₂ | 5a | 20 | 60 | 72 |
| 5 | 4-Cl | 5b | 20 | 60 | 69 |
| 6 | 4-Cl | 5b | 40 | 80 | 65 |
| 7 | 4-Cl | 5b | 20 | rt | 87 |
| 8 | 4-Cl | 5b | 30 | 50 | 71 |
| 9 | 4-OCH ₃ | 5k | 50 | 90 | 62 |
| 10 | 4-OCH ₃ | 5k | 20 | rt | 88 |
| 11 | 4-OCH ₃ | 5k | 20 | 80 | 70 |
| 12 | 4-OCH ₃ | 5k | 40 | 60 | 75 |

Further, in order to establish the role of different catalysts the reaction was performed with various metal salts/hydroxide/oxide viz; CuI, Cu (OAc)₂, Zn (OH)₂, Et₃N, PTSA, Cu₂O. It is inferred from the data presented in **Table 2** that the use of CuI, Cu₂O and Cu (OAc)₂ resulted in the appreciable yield of the final compound. However, the use of CuI resulted in the highest yield. Thus, it was chosen as the catalyst of choice for this transformation. Furthermore, out of different loadings of CuI, maximum yield was obtained with 5mol% of this catalyst (**Table 2**).

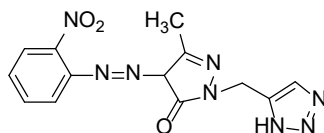
Consequently, with these optimized reaction conditions in hand, a library of 12 differently substituted 1, 2, 3-triazolo-linked pyrazolone compounds was synthesized (**Table 3**).

Table 2. Optimization of catalytic activity for different derivatives(1a-k).

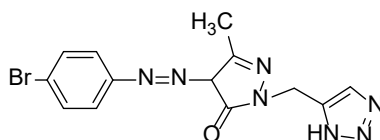
| Entry | Aza compound | R ₁ | R ₂ | Product | Catalyst | Yield (%) |
|-------|--------------|--------------------|------------------|---------|-------------------------------|-----------|
| 1 | 1a | 4-NO ₂ | -CH ₃ | 5a | CuI (5mol %) | 91 |
| 2 | 1a | 4-NO ₂ | -CH ₃ | 5a | CuI (10mol %) | 87 |
| 3 | 1a | 4-NO ₂ | -CH ₃ | 5a | Cu (OAc) ₂ | 78 |
| 4 | 1b | 4-Cl | -CH ₃ | 5b | Zn (OH) ₂ (5mol %) | 50 |
| 5 | 1b | 4-Cl | -CH ₃ | 5b | CuI (5mol %) | 87 |
| 6 | 1b | 4-Cl | -CH ₃ | 5b | Et ₃ N (10mol %) | 58 |
| 7 | 1k | 4-OCH ₃ | -CH ₃ | 5k | CuI (5mol %) | 88 |
| 8 | 1k | 4-OCH ₃ | -CH ₃ | 5k | PTSA (10mol %) | 30 |
| 9 | 1k | 4-OCH ₃ | -CH ₃ | 5k | Cu ₂ O (5mol %) | 55 |

Table 3. Library of synthesized compounds

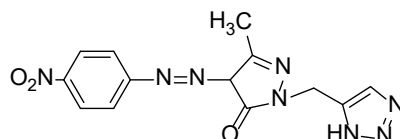
| Entry | Precursor-I | Precursor-II | Product | Time (min.) | Yield (%) |
|-------|-------------|--------------|---------|-------------|-----------|
| 1. | | | | 20 | 91 |
| 2. | 1b | 4b | 5b | 20 | 87 |
| 3. | 1c | 4c | 5c | 20 | 86 |
| 4. | 1d | 4d | 5d | 20 | 84 |
| 5. | 1e | 4e | 5e | 20 | 85 |
| 6. | 1f | 4f | 5f | 20 | 88 |
| 7. | 1g | 4g | 5g | 20 | 84 |
| 8. | 1h | 4h | 5h | 20 | 65 |
| 9. | 1i | 4i | 5i | 20 | 51 |
| 10. | 1j | 4j | 5j | 20 | 81 |
| 11. | 1k | 4k | 5k | 20 | 88 |
| 12. | 1l | 4l | 5l | 20 | 82 |

1-((1*H*-1,2,3-triazol-5-yl)methyl)-3-methyl-4-((2-nitrophenyl)diazenyl)-1*H*-pyrazol-5(4*H*)-one

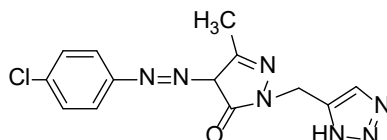
L-1

1-((1*H*-1,2,3-triazol-5-yl)methyl)-4-((4-bromophenyl)diazenyl)-3-methyl-1*H*-pyrazol-5(4*H*)-one

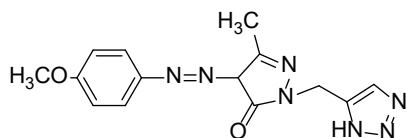
L-2

1-((1*H*-1,2,3-triazol-5-yl)methyl)-3-methyl-4-((4-nitrophenyl)diazenyl)-1*H*-pyrazol-5(4*H*)-one

L-5

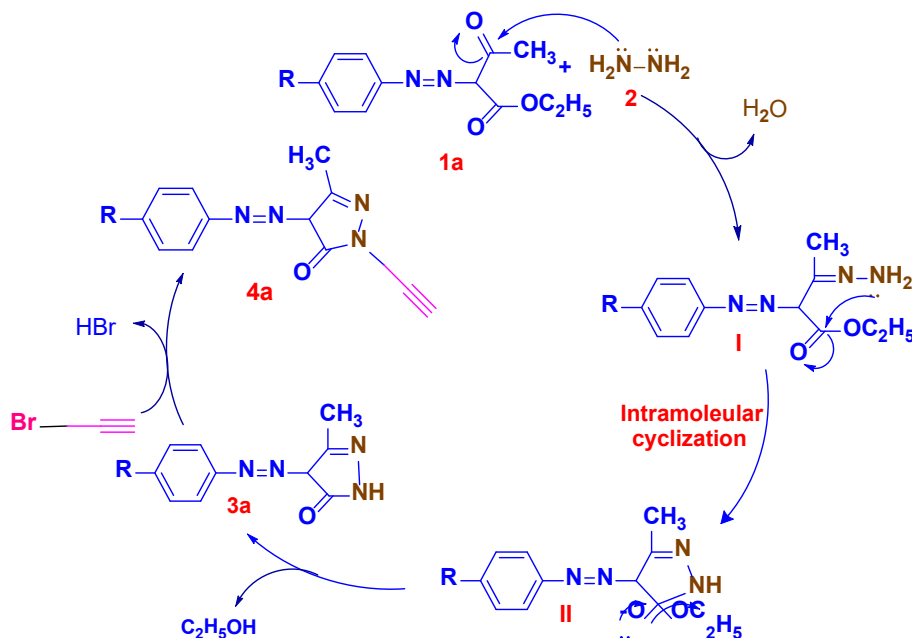
1-((1*H*-1,2,3-triazol-5-yl)methyl)-4-((4-chlorophenyl)diazenyl)-3-methyl-1*H*-pyrazol-5(4*H*)-one

L-3

1-((1*H*-1,2,3-triazol-5-yl)methyl)-4-((4-methoxyphenyl)diazenyl)-3-methyl-1*H*-pyrazol-5(4*H*)-one

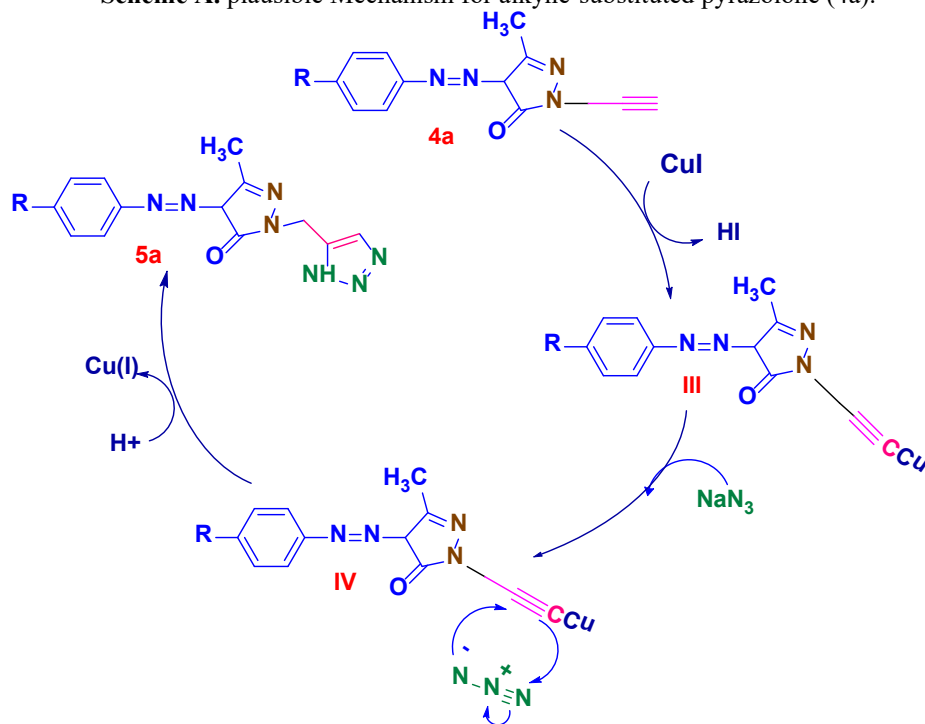
Plausible Reaction Mechanism

The plausible mechanism for the formation of compound **5a** involving CuI was framed according to the literature reports.^{40, 41} The formation of pyrazolone substituted with alkyne as one of the precursors was depicted in **Scheme A**. The reaction proceeds through a nucleophilic attack of hydrazine on the carbonyl carbon atom of ethyl 2-((4-nitrophenyl) diazenyl)-3-oxobutanoate with loss of water molecule. Further, intramolecular nucleophilic attack on carbonyl carbon by another nitrogen atom on the ester functionality with loss of an alcohol molecule resulted in ring closure to pyrazolone nucleus **3a**. Further, the attack of propargyl bromide on pyrazolone resulted in the formation of alkyne-substituted pyrazolone **4a**. The product thus formed was used as one of the substrate precursors to synthesize 1, 2, 3-triazole-linked pyrazolones. The deduced mechanism is delineated in **Scheme B**. The interaction of CuI with terminal alkyne generated copper (I) acetylide **III**. This intermediate undergoes fast cycloaddition with sodium azide followed by protonation and reductive elimination to regenerate the Cu (I) catalyst giving the final product **5a**.



R = $-\text{NO}_2$, $-\text{Cl}$, Br, $-\text{OCH}_3$ etc.

Scheme A. plausible Mechanism for alkyne-substituted pyrazolone (**4a**).



Scheme B. Plausible mechanistic pathway for the synthesis of pyrazolone linked -1, 2, 3-triazole (**5a**).

Visualization plays a crucial role in depicting molecular structures and interactions, enhancing our comprehension of biomolecule relationships and docking simulation outcomes. Docking, as a valuable tool, economizes time and resources by reducing the necessity for experimentation. Furthermore, it efficiently screens numerous compounds, and when coupled with visualization, aids in prioritizing promising candidates. The combined use of docking and visualization offers insights into drug mechanisms and disease pathology. Clear and informative visual representations are essential for effectively interpreting and communicating the results of docking simulations. To address this need, various software tools have been developed. PyMOL-3 is one such tool, offering features for visualizing protein structures and protein-ligand interactions effectively. VMD4 (Visual Molecular Dynamics) provides powerful flexibility in analyzing and visualizing biomolecules, while UCSF Chimera5 focuses on identifying relevant non-covalent interactions. Additionally, Biovia Discovery Studio6 (BDS) is a comprehensive software suite that includes specialized modules for visualizing protein-ligand interactions and conducting in-depth analyses of protein-ligand complexes.⁴²

BDS encompasses a suite of visualization tools for interpreting and communicating the results of molecular simulations and analyses. Key tools within BDS include a 3D Structure Viewer for analyzing protein and small molecule structures, a Ligand Explorer for visualizing interactions between ligands and proteins, a Complex Viewer for visualizing protein-protein and protein-ligand complexes, an Electrostatic Potential Map for illustrating electrostatic potential distribution on a protein surface, and Surface and Volume Rendering for creating detailed and interactive visual representations of molecular structures. These tools empower users to swiftly assess molecular simulation results and make informed decisions in drug discovery. BDS's visualization tools are designed to assist researchers in understanding and communicating the outcomes of molecular simulations, docking studies, and other molecular analyses. This protocol provides guidelines for displaying molecular structures in 3D, emphasizing specific interactions between proteins and ligands, such as hydrogen bonding and hydrophobic interactions, which influence complex stability and binding affinity. BDS's integrated platform consolidates a wide range of molecular modeling and simulation tools, offering a comprehensive solution for drug discovery and molecular biology research. **Table 4** details the results of the molecular docking study obtained for the synthesized compounds with the selected heme-binding protein *P. gingivalis* (PDB ID: 5IAE).

Our docking analyses of L-1 have forecasted the establishment of conventional hydrogen bond interactions (indicated by green dashed lines) with the heme-binding protein of *Porphyromonas gingivalis* (PDB ID: 5IAE) at an energy of -11.0 kcal/mol, involving the residues THRC:140 and TYRC:195. The LYSC:137 residue is anticipated to engage in unfavorable positive-positive stacking, depicted by a red dashed line interaction, with the aromatic ring of the protein. Additionally, it is expected to form pi-anion interactions, represented by orange dashed lines with GLUC:124. Furthermore, attractive charges between the ligand and protein are predicted, illustrated by orange dashed lines.

The docking analyses of L-2 indicate the potential formation of three hydrogen bond interactions with the heme-binding protein of *Porphyromonas gingivalis* (PDB ID: 5IAE) at an energy of -10.1 kcal/mol. These interactions are predicted to occur with the residues ASPC:40 and TYRC:276. Additionally, the TYRC:274 residue is anticipated to engage in pi-pi stacking, as denoted by a purple dashed line, with the aromatic ring of the protein. Furthermore, it is expected to participate in pi-anion interactions, illustrated by gray dashed lines. Lastly, carbon-hydrogen interactions between the ligand and protein are predicted and depicted by blue dashed lines.

Our docking analyses of L-3 have anticipated the occurrence of conventional hydrogen bond interactions (indicated by green dashed lines) with the heme-binding protein of *Porphyromonas gingivalis* (PDB ID: 5IAE) at an energy of -10.6 kcal/mol, specifically involving the LYSC: 137 residues. Additionally, the LYSC: 137 residue is projected to engage in unfavorable positive-positive stacking, depicted by a red dashed line interaction, with the aromatic ring of the protein. Furthermore, it is expected to form pi-alkyl and alkyl bonds, represented by purple dashed lines, with PROC: 201, PHEC: 266, PROA: 201, and PHEA: 266. Alongside, an attractive charge is predicted with GLUC: 124, illustrated by orange dashed lines, between the ligand and protein.

Our docking analysis of L-4 has foreseen the occurrence of conventional hydrogen bond interactions (depicted by green dashed lines) with the heme-binding protein of *Porphyromonas gingivalis* (PDB ID: 5IAE) at an energy of -10.8 kcal/mol, particularly involving the LYSC:137 residue. Additionally, the LYSC: 137 residue is anticipated to partake in unfavorable positive-positive stacking, represented by a red dashed line interaction, with the aromatic ring of the protein. Furthermore, it is expected to establish pi-alkyl and alkyl bonds, illustrated by purple dashed lines, with PROC: 201 and PHEA: 266. Simultaneously, an attractive charge is predicted with GLUC: 124, shown by orange dashed lines, between the ligand and protein.

Our analysis of L-5 docking has predicted the occurrence of conventional hydrogen bond interactions (illustrated by green dashed lines) with the heme-binding protein of *Porphyromonas gingivalis* (PDB ID: 5IAE) at an energy of -11.1 kcal/mol, specifically involving the LYSC: 137 residue. Additionally, the LYSC: 137 residue is expected to engage in unfavorable positive-positive stacking, portrayed by a red dashed line interaction, with the aromatic ring of the protein. Moreover, it is anticipated to form pi-alkyl and alkyl bonds, depicted by purple dashed lines, with PROC: 201, PHEC: 266, PROA: 201, and PHEA: 266. Concurrently, an attractive charge is foreseen with GLUC: 124, as indicated by orange dashed lines, between the ligand and protein.

Table 4. Molecular docking scores of synthesized compounds (1-5) against the heme-binding protein of *Porphyromonas gingivalis* (PDB ID: 5IAE)

| S.No. | Compound | Name | Docking scores/Affinity (kcal/mol) | Ligand- Protein 3D Interactions |
|-------|----------|------|------------------------------------|---------------------------------|
| 1 | | L-1 | -11.0 | |
| 2 | | L-2 | -10.1 | |
| 3 | | L-3 | -10.6 | |
| 4 | | L-4 | -10.8 | |
| 5 | | L-5 | -11.1 | |

According to the docking studies, compounds L-5, L-1 and L-4 have a higher affinity (-11.1, -11.0 and -10.8 respectively) for the target cancer cells than the medication doxorubicin,⁴³ Amoxicillin (-8.6), Moxifloxacin (-8.6), Sulfanilamide (-6), Sulfamethoxazole (-8.1). Therefore, the substances can be regarded as lead compounds for the development of more effective anticancer pharmaceutical agents.

Scheme B suggests a "concerted" nature for the cycloaddition between a cuprum-acetylene complex and azide, implying that the reaction proceeds through a single, simultaneous transition state without intermediates. However, considering the current state of knowledge, it is premature to assume this cycloaddition mechanism a priori. In some instances, alternative stepwise mechanisms involving the formation of zwitterionic or biradical intermediates are possible. These intermediates can significantly influence the reaction pathway and outcome, indicating that the mechanism may vary depending on the specific conditions and substrates involved. Therefore, a thorough investigation is required to definitively determine the mechanistic pathway of such cycloadditions.⁴⁴

3. Conclusion

A new series of 1, 2, 3-triazoles coupled to the pyrazolone nucleus was synthesized using a multi-component click reaction strategy catalyzed by copper. As precursors, a number of arylazo pyrazolones were first synthesized. The sodium azide treatment of the alkenyl pyrazolone was then permitted in the copper-catalyzed click reaction mode. A variety of substituted triazoles can be synthesized using the developed method with good yields. This protocol offers several benefits, including easy work-up procedures, quick reaction times, and mild experimental conditions. Additionally, the environmentally friendly green synthetic protocol benefited from the base-free and additive-free synthetic approach. Compounds L-5, L-1, and L-4 have a higher affinity for the target cancer cells (-11.1, -11.0 and -10.8 respectively) than do drugs like doxorubicin, amoxicillin (-8.6), levofloxacin (-8.6), sulfanilamide (-6), and sulfamethoxazole (-8.1). As a result, these compounds listed above can be thought of as lead compounds for the creation of pharmaceuticals that are more potent against cancer.

Supporting Information Summary

Experimental procedure and spectroscopic data are available in supporting information.

Acknowledgment

The authors express gratitude to CSIR, Delhi (File No: 09/301(0135)/2018-EMR-I) for the Junior Research Fellowship. Additionally, appreciation is extended to the Sophisticated Analytical Instrumentation Facility at Punjab University, Chandigarh, for supplying experimental results.

Conflict of Interest

The authors confirm that this article's content has no conflict of interest.

References

1. Boyang Yin 1, Céline Croutxé-Barghorn, Christelle Delaite 1, Xavier Allonas. (2019) A new synthetic pathway based on one-pot sequential aza-Michael addition and photo CuAAC click reactions. *RSC Adv.*, 9, 4824-4831.
2. Yang Na., Yuan G., (2018) A Multicomponent Electrosynthesis of 1,5-Disubstituted and 1-Aryl 1,2,4-Triazoles. *J. Org. Chem.*, 83, 19, 11963–11969
3. Tornøe C. W., Christensen C., Meldal M., (2002) Peptidotriazoles on Solid Phase: [1,2,3]-Triazoles by Regiospecific Copper(I)-Catalyzed 1,3-Dipolar Cycloadditions of Terminal Alkynes to Azides. *J. Org. Chem.*, 67, 3057-3064.
4. Liang L, Astruc D., (2011) The copper (I)-catalyzed alkyne-azide cycloaddition (CuAAC) "click" reaction and its applications. An overview. *Coor. Chem. Rev.* 255, 2933-2945.
5. Yamada M., Matsumura M., Uchida Y., KavaHata M., Murata Y., Kakusava N., Yamaguchi K., Yasuike S., (2016) Copper-catalyzed [3 + 2] cycloaddition of (phenylethynyl)di-p-tolylstibane with organic azides. *Beilstein J. Org. Chem.* 12, 1309–1313.
6. Galstya S., Ghochikyan V., Frangyan R., Tamazyan A., Ayvazyan G., (2018) Synthesis of Novel Derivatives of 1,2,4-Triazoles. *Chemistry select*, 3, 9981-9985.
7. Cera G., Haven T., Ackermann L., (2013) Versatile reactivity of rhodium-iminocarbenes derived from N-sulfonyl triazoles. *Angew. Chem., Int. Ed.*, 52, 1371-1373.
8. Ackermann L., Jeyachandran R., Potukuchi H. K., Novak P., Buttner L., (2010) Palladium-Catalyzed Dehydrogenative Direct Arylations of 1,2,3-Triazoles. *Org. Lett.*, 12, 2056.
9. Li H., Wu X., Hao H., Li H., Zhao Y., Wang Y., Lian P., Zheng Y., Bao X., Wan X., (2018) [3+2] Cycloaddition of Nitrile Ylides with Diazonium Salts: Copper Catalyzed One Pot Synthesis of Fully Substituted 1,2,3-Triazoles. *Org. Lett.*, 20, 5224-5227.

10. Bechara W. S., Khazhieva I. S., Rodriguez E., Charette A. B., (2015) One-Pot Synthesis of 3,4,5-Trisubstituted 1,2,4-Triazoles via the Addition of Hydrazides to Activated Secondary Amides. *Org. Lett.*, 17, 1184-1187.
11. Kolb H. C., Finn M. G., Shapless K. B., (2001) Click Chemistry: Diverse Chemical Function from a Few Good Reactions. *Angew. Chem. Int. Ed.*, 40, 2004-2021.
12. Rostovtsev V. V., Green L. G., Folkin V. V., Sharpless K. B., (2002) A Stepwise Huisgen Cycloaddition Process: Copper(I)-Catalyzed Regioselective "Ligation" of Azides and Terminal Alkynes. *Angew. Chem. Int. Ed.*, 41, 2596.
13. Prieto A., Uzel A., Bouyssi D., Monteiro N., (2017) Thiocyanation of N, N -Dialkylhydrazonoyl Bromides: An Entry to Sulfur-Containing 1,2,4-Triazole Derivatives. *Eur. J. Org. Chem.*, 28, 4201-4204.
14. Szabo K. E., Pahi A., Somsak L., (2017) C-Glycosyl 1,2,4-triazoles: Synthesis of the 3- β -d-glucopyranosyl-1,5-disubstituted and 5- β -d-glucopyranosyl-1,3-disubstituted variants. *Tetrahedron.*, 73, 3810-3822.
15. Holm S. C., Straub B. F., (2011) Synthesis of N-Substituted 1,2,4-Triazoles A Review. *Org. Prep. Proced. Int.*, 43, 319-347.
16. Rostovtsev V. V., Green L.G., Fokin V. V., Sharpless K. B., (2002) A Stepwise Huisgen Cycloaddition Process: Copper(I)-Catalyzed Regioselective "Ligation" of Azides and Terminal Alkynes. *Angew. Chem. Int. Ed.*, 41, 2596-2599.
17. Johan R. J., Tamás B. S., Anna S. S., Nina K. (2016) Ruthenium-Catalyzed Azide Alkyne Cycloaddition Reaction: Scope, Mechanism, and Applications. *Chem. Rev.* 116, 23, 14726-14768.
18. Yang N., Yuan G., (2018) A Multicomponent Electrosynthesis of 1,5-Disubstituted and 1-Aryl 1,2,4-Triazoles. *J. Org. Chem.*, 83, 11963-11969.
19. Bechara W. S., Khazhieva I. S., Rodriguez E., Charette A. B., (2015) One-Pot Synthesis of 3,4,5-Trisubstituted 1,2,4-Triazoles via the Addition of Hydrazides to Activated Secondary Amides. *Org. Lett.*, 17, 1184-1187.
20. Malani H. A., Makwana A. H., Makwana H., (2017) A brief review article: Various synthesis and therapeutic importance of 1, 2, 4-triazole and its derivatives. *Mor. J. Chem.* 5, 41- 58.
21. Mohammad B., Rahele D., Mahdi M., Khosro J., (2017) Synthesis of new 2-substituted pyrazolo[5,1-b] [1,3] oxazoles via Sonogashira coupling reactions in water. *Tetrahedron.*, 73, 3281-3287.
22. Fustero S., Sanchez-Rosselo M., Barrio P., Simon-Fuentes A., (2011) From 2000 to mid-2010: a fruitful decade for the synthesis of pyrazoles. *Chem. Rev.*, 111, 6984-7034.
23. Li R. Y., Li C., Li J. C., (2015) Synthesis and biological evaluation of 1,3-diaryl pyrazole derivatives as potential antibacterial and anti-inflammatory agents. *Bioorg. Med. Chem. Lett.*, 25, 5052-5057.
24. Kamal A., Saik A., B., Jain N., (2015) Design and synthesis of pyrazole-oxindole conjugates targeting tubulin polymerization as new anticancer agents. *Eur. J. Med. Chem.*, 92, 501-513.
25. Alegaon S., G., Alagawadi K., R., Garg M., Dushyant K., Vinod D., (2014) 1,3,4-Trisubstituted pyrazole analogues as promising anti-inflammatory agents. *Bioorg. Chem.*, 54, 51-59.
26. Kunes J., Balsanec V., Pour M., Buchta V., (2001) Synthesis and Antifungal Activity Evaluation of 3-Hetaryl-2,5-dihydrofuran-2-ones. An Unusual Fragmentation of the Oxazole Ring via 2,3-Selenoxide Shift Czech. *Chem. Commun.*, 66, 1809-1830.
27. Daswani U., Singh U., Sharma P., Kumar A. (2018) From Molecules to Devices: A DFT/TD-DFT Study of Dipole Moment and Internal Reorganization Energies in Opto electronically Active Aryl Azo Chromophores. *J. Phys. Chem. C*, 122, 14390-14401.
28. Ahuja M., Biswas S., Sharma P., Samanta S., (2018) Metal-Free Based Domino Approach to Pyrano-Fused-Pyrido[3,2,1-jk] carbazolones: Antibacterial and Molecular Docking Studies. *chemistry select*, 3, 4354-4360.
29. Malvia H., Kumar A., Sharma P., Mishra R., (2017) A Submicellar Liquid Chromatographic Method for Quantitative Determination of Muscle Relaxant Drug Baclofen in Solubilized System. *asian journals of chemistry*, 29, 1509-1514.
30. Malvia H., Sharma A., Sharma P., Mishra R., (2017) A Micellar Liquid Chromatographic Method for the Determination of Azosemide in Solubilized System. *J. Surfact. Deterg.*, 20, 1411-1418.
31. Sharma A., Sharma P., Sharma P. K., (2017) Exploration of Antioxidant Activity of Newly Synthesized Azo Flavones and its Correlation with Electrochemical Parameters along with the Study of their Redox Behaviour. *Journal of analytical chemistry*, 72, 1034-1044.
32. Reen G. K., Kuma A., Sharma P., (2017) In vitro and in silico evaluation of 2-(substituted phenyl) oxazolo [4,5-b]pyridine derivatives as potential antibacterial agents. *Med. Chem. Res.*, 26, 3336-3344.
33. Reen G. K., Ahuja M., Kumar A., Patidar R., Sharma P., (2017) ZnO Nanoparticle-Catalyzed Multicomponent Reaction for the Synthesis of 1,4-Diaryl Dihydropyridines. *Organic Preparation and Procedures International*, 49, 273-286.
34. Reen G. K., Kumar A., Sharma P., (2019) Recent advances on the transition-metal-catalyzed synthesis of imidazopyridines: an updated coverage. *Beilstein. J. Org. Chem.*, 15, 1612-1704.
35. Orazio A. A., Gianfranco F., Paolino F., Fabio M., Giada M., Francesca R. P., (2010) Copper (II)/Copper (I)-Catalyzed Aza-Michael Addition/Click Reaction of in Situ Generated α -Azidohydrazones: Synthesis of Novel Pyrazolone-Triazole Framework. *Org. Lett.*, 12, 468-471.
36. Dresler E., Woliński P., Wróblewska A., Jasiński R., (2023) On the Question of Zwitterionic Intermediates in the [3+2] Cycloaddition Reactions between Aryl Azides and Ethyl Propiolate. *Molecules*, 28, 8152.

37. Maleki A., Rahimi J., Demchuk O. M., Wilczewska A. Z., Jasiński R., (2018) Green in water sonochemical synthesis of tetrazolopyrimidine derivatives by a novel core-shell magnetic nanostructure catalyst. *Ultrasonics Sonochemistry*, 43, 262-271.
38. Jasinski R., (2015) Nitroacetylene as dipolarophile in [2 + 3] cycloaddition reactions with allenyl-type three-atom components: DFT computational study. *Monatsh Chem.*, 146 591–599.
39. Tornøe, C. W., Christensen, C., Meldal, M. (2002). Peptidotriazoles on Solid Phase: [1,2,3]-Triazoles by Regiospecific Copper(I)-Catalyzed 1,3-Dipolar Cycloadditions of Terminal Alkynes to Azides. *The Journal of Organic Chemistry*, 67(9), 3057-3064. DOI: 10.1021/jo011148j.
40. Weiguo W., Yunzhi L., Yudao M., Chen-Ho T., Zhenghu X., (2018,) Copper (I)-Catalyzed three-component click/persulfuration cascade: Regioselective synthesis of triazole disulfides. *Org. Lett.* 20, 2956-2959.
41. Orazio A. A., Gianfranco F., Paolino F., Fabio M., Giada M., Francesca R. P. (2010) Copper (II)/Copper (I)-Catalyzed Aza-Michael Addition/Click Reaction of in Situ Generated α -Azidohydrazones: Synthesis of Novel Pyrazolone– Triazole Framework. *Org. Lett.*, 12, 468-471.
42. Trott O., Olson A. J., (2010) AutoDock Vina: improving the speed and accuracy of docking with a new scoring function, efficient optimization, and multithreading. *Journal of Computational Chemistry* 31, 455-461. DOI 10.1002/jcc.21334
43. Dongamanti A. Gugulothu T. Bhukya K. K., Gundu S., Dharavath R., Thumma V., Madderla S., Bujji S., (2023) Microwave-assisted synthesis, molecular docking studies of 1,2,3-triazole-based carbazole derivatives as antimicrobial, antioxidant and anticancer agents., *RSC Adv.*, 13, 25, DOI: 10.1039/d2ra05960frsc.li/rsc-advances
44. Jasinski R., Dresler E., (2020) On the Question of Zwitterionic Intermediates in the [3+2] Cycloaddition Reactions: A Critical Review. *Organics*, 1, 49–69.



© 2025 by the authors; licensee Growing Science, Canada. This is an open access article distributed under the terms and conditions of the Creative Commons Attribution (CC-BY) license (<http://creativecommons.org/licenses/by/4.0/>).